

Morphology engineering of ZnO nanostructures

Volodymyr Khranovskyy and Rositsa Yakimova

Linköping University Post Print

N.B.: When citing this work, cite the original article.

Original Publication:

Volodymyr Khranovskyy and Rositsa Yakimova, Morphology engineering of ZnO nanostructures, 2012, Physica. B, Condensed matter, (407), 10, 1533-1537.

<http://dx.doi.org/10.1016/j.physb.2011.09.079>

Copyright: Elsevier

<http://www.elsevier.com/>

Postprint available at: Linköping University Electronic Press

<http://urn.kb.se/resolve?urn=urn:nbn:se:liu:diva-77524>

Morphology engineering of ZnO nanostructures

V. Khranovskyy* and R. Yakimova

Department of Physics, Chemistry and Biology (IFM), Linköping University, 58183
Linköping, Sweden

*Corresponding author.

e-mail address: volkh@ifm.liu.se

tel: +46-13-282663

fax: +46-13-137568

Abstract

The nanosized ZnO structures were grown by atmospheric pressure metalorganic chemical vapor deposition (APMOCVD) at the temperature range 200 – 500 °C at variable precursor pressure. The temperature induced evolution of the ZnO microstructure was observed, resulting in regular transformation of the material from conventional polycrystalline layers to hierarchically arranged sheaves of ZnO nanowires. The structures obtained were uniformly planarly located over the substrate and possessed as low nanowires diameter as 30 – 45 nm at the tips. The observed growth evolution is explained in term of ZnO crystal planes free energy difference and growth kinetic. For comparison, the convenient growth at constant precursor pressure on Si and SiC substrates has been performed, resulted in island-type grown ZnO nanostructures. The demonstrated nanosized ZnO structures may have unique possible areas of application, which are listed here.

PACS keywords

ZnO nanostructures, APMOCVD, temperature evolution

1. Introduction

Engineering of the crystal's morphology and microstructure has initiated great research interest. Particularly control of the shapes, size and morphology of novel or mature functional materials is of high interest, enabling manifestation of their novel properties or tailorable functions. Zinc oxide is a promising II–VI semiconductor, having wide band gap ~ 3.37 eV and a large exciton binding energy ~ 60 meV at room temperature. It has attracted increasing interest due to its potential applications in electronics [1], photonics [2], sensors [3], transistors [4], field emission displays [5], etc. It is one of the most gifted materials for the fabrication of short-wavelength optoelectronic devices including blue-UV light-emitting and room temperature UV lasing diodes [6]. ZnO possesses one of the richest family of nanostructures: various nanorods, nanopillars, nanowires, nanodons, nanodrums, nanopropellers, nanonails, nanobridges etc. have been widely reported in literature [7]. However, such exotic morphologies of ZnO nanostructures complicate their functionality, i. e. hamper their practical applications, while the controllable growth of ordered and uniform ZnO nanostructure is highly desirable and may enable their possible applications in various devices. Particular interest represents the hierarchical ZnO nanostructures, being able to combine the high surface-to-volume ratio and fundamental material properties of ZnO, which may be essential for specific applications such as gas- and bio- sensors, hybrid solar cells, etc [8]. Recently, we have demonstrated the ability to grow well-ordered ZnO nanopillars on a seeding layer via selective homoepitaxial growth by atmospheric pressure metalorganic chemical vapor deposition (APMOCVD) [9]. Moreover, by this technique we succeeded in obtaining ZnO nanostructures of diverse morphology. Clear evolution of the

texture and microstructure of ZnO nanostructured material was observed within the growth temperature range (200 – 500 °C). Here, we report the observed substrate temperature effect on the ZnO nanostructures growth within the applied growth procedure.

2. Experimental

The ZnO nanostructures were grown by APMOCVD technique by using Zn (AcAc)₂ as a precursor. The precursor was loaded into an evaporator, and its pressure was controlled via changing the evaporator temperature (130 – 220 °C). The substrates were distanced from the evaporator and were located in the deposition zone. The growth chamber was pre-evacuated and filled by buffer Ar gas in a multy-step way. Standard Si (100) substrates were used, being cleaned in acetone and ethanol for 10 minutes and dried by N flow afterwards. The total growth time was around 30 minutes. More details about the APMOCVD growth of ZnO nanostructures can be found elsewhere [9, 10].

Two sets of samples were prepared, aiming to investigate the temperature, precursor's pressure and possible substrate effect on the structure and morphology of ZnO nanostructures. First, ZnO samples were prepared at a variable precursor supersaturation (set 1) at the substrate temperature ranged 200 – 500 °C. Samples were located simultaneously in the growth chamber; being subjected to the existed temperature gradient in the growth zone. Second, the ZnO nanostructures were deposited under constant low supersaturation (low ZnO precursors pressure) and constant growth temperature 450 °C; two substrates (Si (100) and 4H:SiC (0001), 4° off-cut) were used simultaneously.

The grown structures were characterized in terms of their structural properties by x-ray diffraction (XRD) via θ -2 θ scans using a Philips PW 1825/25 diffractometer, utilizing Cu-K α radiation ($\lambda = 0.1542$ nm). The microstructure of the nanostructures was studied by scanning electron microscopy (SEM) using a Leo 1550 Gemini SEM operated at voltages ranging from 10 to 20 kV and using a standard aperture value of 30 μ m.

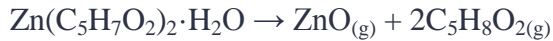
3. Results and discussions

3.1 Precursors chemistry

The grown material structural, electrical and optical properties are strongly affected by the precursors used. Zinc acetylacetonate (ZnAcAc)₂ is a convenient zinc oxide precursor for the vapor transport method, such as CVD [11,12] and is an alternative for the mainly used zinc precursors diethylzinc (DEZ-Zn(C₂H₅)₂) or dimethylzinc (DMZ - Zn(CH₃)₂). As a solid state precursor, it has low sublimation temperature and high vapor pressure [13]. Moreover, it is a single source precursor, which means that it provides both zinc and oxygen species via decomposition. This eventually provides constant stoichiometry content of ZnO, which may be considered as an encouraging premise for p-type ZnO attainment. Both pure and doped ZnO material may be prepared via respective mixture of (ZnAcAc)₂ with acetylacetonates of other elements (Ga, In, Al, Mg, Cd), accessible commercially [14]. The low toxicity of (ZnAcAc)₂ by itself as well as the products of its decomposition enable to consider it as environmental and human friendly source for ZnO growth [15].

The thermal decomposition of the (ZnAcAc)₂·H₂O has been studied since 1960s, when it was found that the main decomposition product when heated at 130 °C was gaseous acetylacetone (C₅H₈O₂) [16]. Fiddes et al. reported that at temperatures below 200 °C the decomposition of Zn(AcAc)₂ in wet conditions is due to a combination of exothermic intramolecular and intermolecular processes while at temperatures above 200 °C a water enhanced pyrolysed mechanism is likely active [17]. Arii et al. reported a lowering of the decomposition temperature in a high water vapor pressure environment and suggest that

crystalline ZnO can be synthesized at temperatures as low as 11 °C via the following simplified decomposition scheme [18]:



Fauteux et al. recently demonstrated that laser-induced decomposition of the $\text{Zn}(\text{AcAc})_2$ resulted in the ZnO nanostructures formation [19]. It has successfully being used in MOCVD growth process to grow aligned hexagonal nanorods and whiskers, nanotube arrays and thin films at temperature range 500 – 650 °C on various substrates [20]. Earlier, we have reported successful growth of pure ZnO and Ga doped films even at lower substrate growth temperatures ($T = 250$ °C) by PEMOCVD [21, 22]. It was concluded that the plasma discharge promotes the precursors decomposition and increases the ZnO adatoms mobility, resulting in high quality film formation [23] at lowered temperatures. Recently the integration of the ZnO nanostructures with Si and SiC via APMOCVD has been reported to result in advanced structural and optical properties [24, 9]. Here, we applied varying precursor pressure for growth of ZnO nanostructures. Such a growth approach resulted in a diverse ZnO nanostructures morphology, depending on the substrate temperature.

3.2 Effect of the substrate temperature on the ZnO microstructure

The evolution of the nanostructures morphology with a temperature increase was complementary studied by SEM and XRD techniques. Distinctive feature is that the nanostructures morphology changes systematically with the temperature, driven by ZnO crystal planes anisotropy and obeying the crystal growth theory. The general explanation for the morphology of the ZnO nanostructures is related to the difference in the surface free energies for the main crystallographic planes of hexagonal ZnO: $G_{001} = -2.8102$ kJ/mol, $G_{101} = -2.1067$ kJ/mol and $G_{100} = -2.0013$ kJ/mol, respectively. Due to this anisotropy, preferential growth on the plane of lowest energy occurs, providing the elongated ZnO structures along the c-axis [25]. However, at lowered temperature the polycrystalline film, containing grains oriented toward all above described planes can be obtained. The temperature evolution of the XRD spectra of the nanostructures is presented on figure 1. ZnO, grown at low temperatures is of polycrystalline nature – the reflection peaks of planes (100), (002), (101) and even (102) are present along with the Si substrate reflection peak (Fig. 1a,b,c). With further temperature increase the reflection of the plane (002) becomes most strong, being totally dominating for the structures grown at highest temperature (Fig. 1c,e,f).

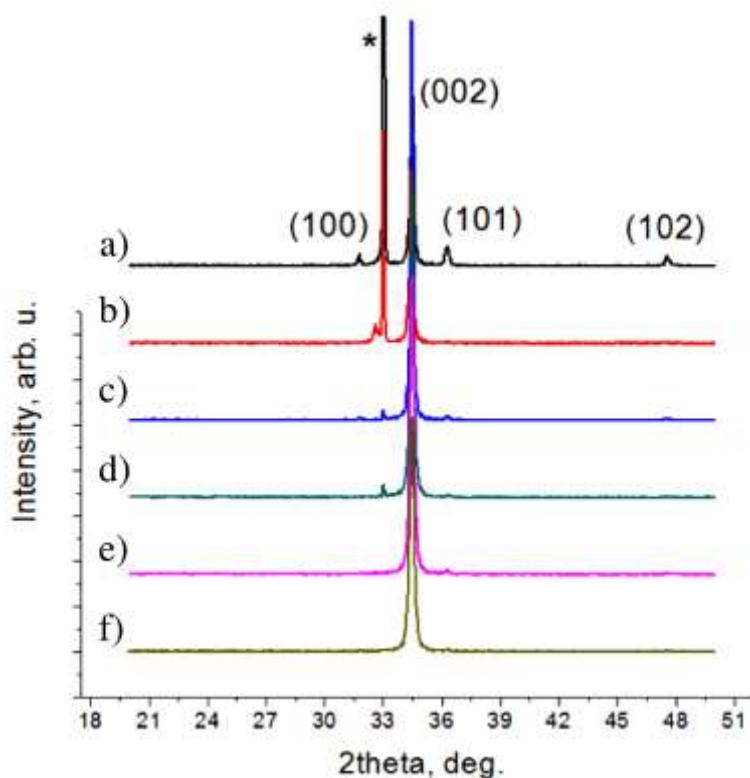


Figure 1. The XRD patterns of ZnO nanostructures grown at set 1 conditions and respective substrate temperature ranges: a - corals (200 – 240 °C); b - cabbages (240 – 280 °C); c - porous hexagons (280 - 320 °C); d - bundles (320 – 365 °C); e - sheaves (365 – 415 °C); f - open sheaves (415 – 525 °C). The respective reflections of the crystallographic planes are indicated. The substrate peak is marked as “*”.

SEM analysis confirms the XRD data – the images of the obtained structures are presented at figure 2a-f. Structures, grown within the temperature range 200 – 240 °C – “corals” - are the blocks of the elongated ZnO nanocrystallites (Fig. 2a). The elongated shape of crystals results from the distinctive anisotropic growth of ZnO – toward (001), (100) and (101) planes. The SEM image correlated with the XRD spectra of the corals: the peaks, related to the respective planes are observed. No other peaks were observed, which proves the homogeneity of the ZnO material and single ZnO phase obtained. Such growth morphology can be explained as following: independently of the precursor pressure, at low temperatures the species of the substrate surface have low diffusion ability, thus tend to freeze rapidly upon reaching the surface. Along with the high nucleation density, what is peculiar for low temperature epitaxy, the corals are randomly located over the substrate without prominent texture. The lateral size of the corals is around 1 - 2 μm .

With the temperature increase from 240 to 280 °C, the corals evolve into the shape of cabbage – having a number of “leaves” and a core in the centre (Fig. 2b). The core of the nanostructure has the hexagonal shape, which implies that the original nuclei is a single crystalline ZnO grain, which is epitaxially grown on the Si substrate, having the *c*-plane parallel to the surface. Moreover, at this stage the nanostructures start to be textured toward the substrate. Even within the temperature range, the texture along the *c*-axis is improved

and more cores are oriented with their c-plane parallel to the substrate. This is confirmed by the XRD spectrum of the ZnO “cabbages”: the peak, related to the (0001) plane is more intense, although the other two peaks are present, related to the respectively (10-10) and (10-11) planes. The characteristic size of the “cabbages” is around 1.5 – 2 μm .

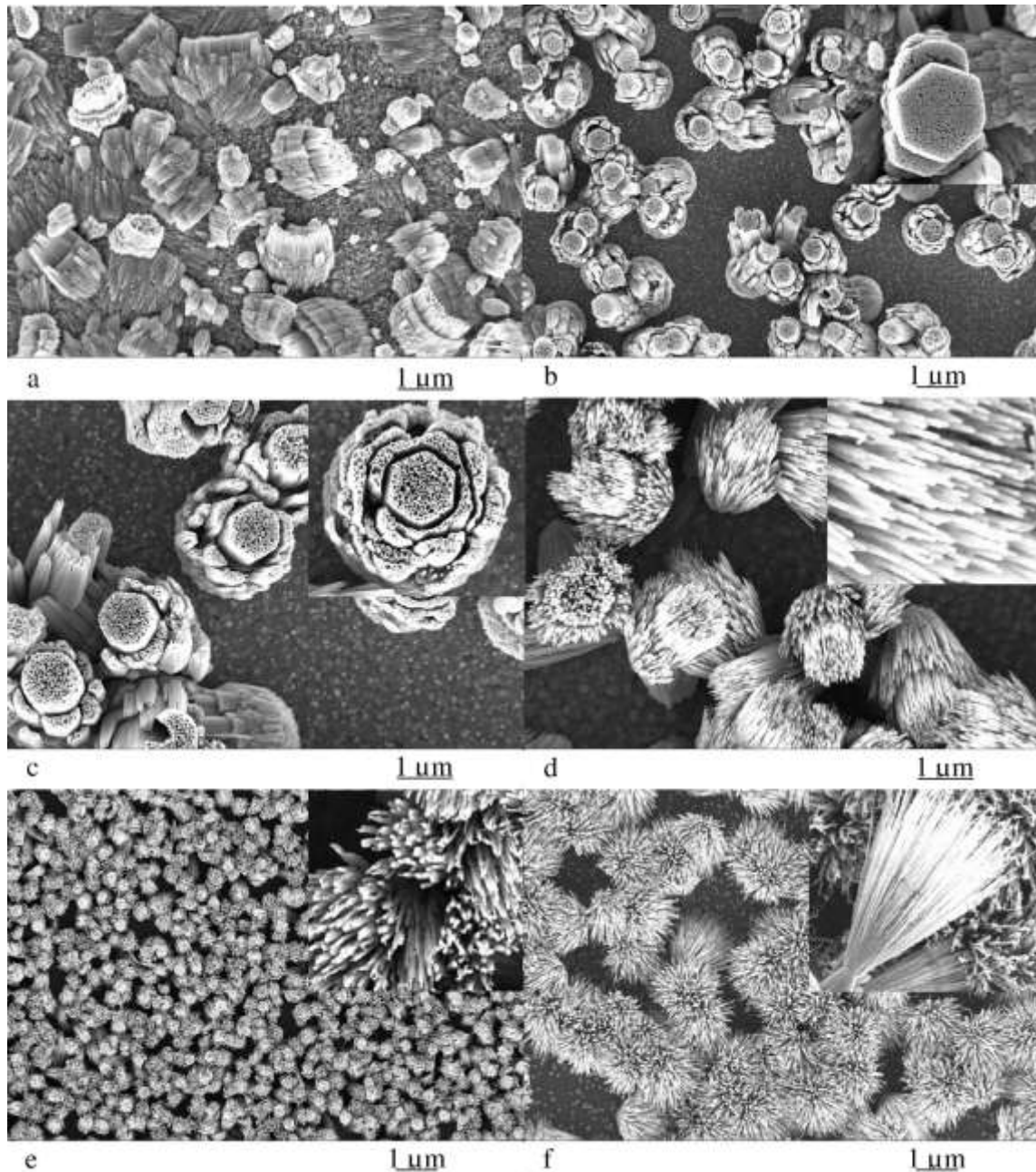


Figure 2. The SEM images of ZnO nanostructures grown at set 1 conditions and respective substrate temperature ranges: a - corrals (200 – 240 °C); b - cabbages (240 – 280 °C); c - porous hexagons (280 - 320 °C); d - bundles (320 – 365 °C); e - sheaves (365 – 415 °C); f - open sheaves (415 – 525 °C). The insets represent respective enlarged images of the features.

At further temperature increase up to 320 °C most of the cabbage-like structures are well textured. Moreover, under thorough examination, the core hexagons were found to have nanosized pores along their c-axis. We explain such an effect as the results of preferential growth along the c-axis, thus resulting in creation of the walls with elongated pores between them (Fig. 2c). The size of the porous crystals do not deviate much from that of the cabbages structures - 1.5 – 2 μm. The diameter of the pores were around 20 – 40 nm for the growth temperature 280 °C and was found to increase with increasing temperature, reaching 60 – 80 nm at the growth temperature 320 °C. The XRD spectrum of the porous hexagons reveal their high texture along the c-axis, with the intense peak of reflection from the (0001) plane relative to the other reflections.

At the temperature 335 °C the nanostructures undergo a qualitative shape change: the nanoporous hexagons transform into bundles of ZnO nanorods (Fig. 2d). The diameter of the nanorods is around 30 – 50 nm at the tips increasing slightly approaching their roots. Interestingly, the nanorods in the bundles are arranged in a hexagonal shape. We believe that with the temperature increase, the nanowalls are transformed into nanorods, losing the connections in between them. The XRD θ - 2θ spectra prove the high crystalline orientation of the nanorods, with a single peak, related to the (0001) reflection.

Further increase of the temperature causes a transformation of the bundles into sheaves of nanorods, along with a slight decrease of their diameter, narrowing of their bunching zone and losing their hexagonally ordered arrangement (Fig. 1e). At this stage the presence of double-side sheaves is observed. Their appearance can be explained due to the presence of (0001) plane twinned ZnO crystals, being further developed into sheaves toward the opposite direction. The sheaves are densely located over a large surface area and are textured along the c-axis of ZnO, which is in agreement with the XRD data (Fig. 1e). The further temperature increase just improves their c-axis texture (Fig. 1f). Finally, at high temperatures, the sheaves of the nanorods are still highly oriented and perfectly located, however their surface is rough. That can be a result of the Zn and O species re-evaporation during the growth, what is expected for ZnO and was earlier observed for growth temperatures over 500 °C [26].

The summary of the structural and morphological properties of ZnO nanostructures, grown at different temperatures is presented in Table 1.

Table 1. Description of the morphology shape and structural features of ZnO nanostructures depend on the growth temperature

Growth temperature range, °C	$2\theta_{(hkl)}$, (degrees)	Crystal planes (<i>h k l</i>)	XRD FWHM, (degrees)	XRD Intensity (<i>h k l</i>), a. u.	Morphology	Characteristic size
200 – 240	31.76	(100)	0.3	45	Corals	1 – 2 μm
	34.47	(002)	0.2	954		
	36.29	(101)	0.24	80		

240 – 280	32.5	(100)	0.21	68	Cabbages	1.5 – 2 μm / pores around 15 – 40 nm
	34.46	(002)	0.16	1366		
	36.33	(101)	0.19	6		
280 – 320	34.48	(002)	0.14	1761	Porous hexagons	1.5 – 2 μm / pores around 20 – 80 nm
	36.3	(101)	0.18	22		
320 – 365	34.48	(002)	0.23	1426	Bundles	1.5 – 2 μm / 30 – 50 nm at the tips
365 – 415	34.48	(002)	0.24	1321	Sheaves	1 – 1.2 μm / 30 – 40 nm
415 – 525	34.466	(002)	0.27	1033	Open sheaves	1 μm / 20 – 30 nm

3.2. ZnO nanostructures, grown at low precursor pressure

We investigated the ZnO nanostructures, grown at low supersaturation onto Si and SiC substrates at constant substrate temperature of 450 °C. The growth resulted in the deposition of well shaped ZnO crystallites over the substrate surface (Fig. 3a, b). Obviously, at low flux of precursors and at high enough temperatures, the ZnO adatoms possess high diffusivity over the surface, enabling creation of well faceted crystals. The crystals of diverse morphology are observed, however several general shapes can be outlined. The ZnO nanostructures on Si substrates consist of hexagonal structures (prisms and pyramids), differently located on the surface (perpendicular or parallel to the surface) and their mixed complexes, as a results of multi-nucleation. The hexagonal geometry of ZnO nanostructures is due to the self texture character of growth, resulting in their c-axis texture. However, the formation of pyramids, located parallel to the substrate may be due to the substrate dictated growth. ZnO and Si have different crystal structures (one hexagonal wurtzite structure, the other fcc diamond), and the lattice parameter mismatch is essential: $a = 0.32495$ nm, $c = 0.52069$ nm for ZnO; $a = 0.54305$ nm for Si. The in-plane lattice mismatch for ZnO aligned with the c-axis perpendicular to the Si surface is as high as 40.16%. However, at the growth of ZnO with the c-axis parallel to the Si substrate surface, providing the epitaxial relationship $\text{ZnO}_{(100)} \parallel \text{Si}_{(100)}$ lattice mismatch becomes only $\approx 4\%$. This explains why some of the ZnO structures are located with their c-axis parallel to the substrate surface.

The drum-shaped ZnO nanostructures are made up of hexagonally faceted twinned-crystals having flat surfaces on both the ends (Fig. 3a). The crystals are twinned on the (0001) plane. The hexagon-pyramids are expected to have the same formation mechanism.

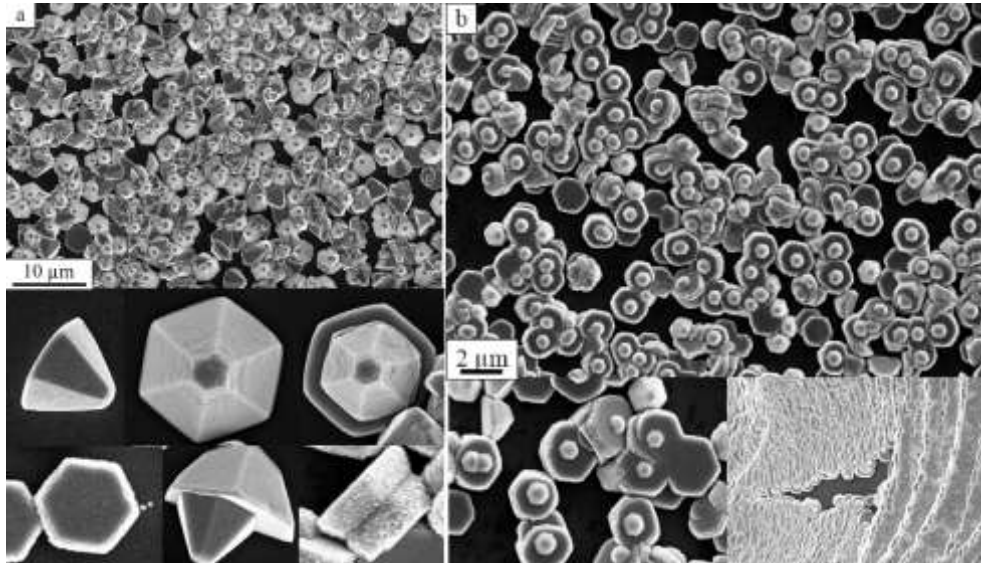


Figure 3. ZnO nanostructures, grown at low precursor pressure on Si (a) and SiC (b) at 450 °C.

The growth on SiC substrate agrees well with the explanation above: the hexagons with *c*-axis perpendicular to the SiC surface are dominant. For ZnO SiC is an attractive substrate material, mainly due to the similarity of the crystal structures and small lattice and thermal expansion coefficient mismatch: $a_{6H-SiC} = 0.308$ nm, $TEC_{6H-SiC} = 4.3 \times 10^{-6}/K$, while $a_{ZnO} = 0.3252$ nm, $TEC_{ZnO} = 6.51 \times 10^{-6}/K$, giving a misfit in the basal plane $\sim 5.4\%$. The small lattice mismatch of ZnO and SiC, along with the texture dictated growth mode results in the *c*-textured massive growth of nanostructures. Also, it was observed that the ZnO tends to coalesce together, resulting in mosaic structured layer of ZnO on SiC (Fig. 3b). The ZnO hexagons tend to decorate the substrate defects (edges, scratches), which is due to the preferred nucleation on them. We believe that the fact that SiC substrate is 4° off-cut favours the nucleation of ZnO nanocrystals and their epitaxial growth. Earlier we reported in details the growth of ZnO HEX on SiC substrates, assisted by high quality hetero interface and advanced optical properties [24]. We suppose, that the observed features provide the necessary premise for the epitaxial growth of high quality ZnO nanostructures on SiC for unique applications.

4. Application aspects

The grown structures have large potential for different low-scale oriented applications and demand a thorough evaluation. First of all, the nanoporous ZnO structures, having a high surface area, can be used as adsorbents or catalysts. The potential field for the porous ZnO nanostructures may be the gas storage, separation or molecular catalysis. Moreover, sensing or removing toxic, harmful or oxidizing gases (such as CO, NO_x, O₂ and so on) using nanoporous materials is currently of great importance because of industrial and environmental demands [27, 28]. Furthermore, if it is possible to activate a nanopore surface by external stimuli where and when desired, on-demand gas storage/trapping systems can be realized [29]. Thus, functionalization of the ZnO nanopores structures may be the forthcoming challenge. The ZnO bundles and sheaves, being in fact unique hierarchical structures, are suggested to have potential in many device applications. Since they are

aligned and oriented toward the surface, so they can be used as conventional ZnO nanoarrays in nanosensors or field emitters. Because of their unique multi-forked structure, they may be used as nanotweezers to capture nanoparticles or other nanostructures. Since both the bundles and sheaves originate from the micro-sized grain, it can be possible to handle and manipulate by them, which is a great advantage for them as a nanotweezers or other nanotools. Demonstrated growth of ZnO on SiC creates significant premises for design of heterostructures, which are considered to be the main elements of the conventional, or nanosized short-wavelength light emitting devices and lasers (LEDs and LDs). Since the SiC is the approved alternative substrate for ZnO, the achievement of high quality ZnO growth on p-type SiC is a valuable task.

6. Conclusions

The APMOCVD growth of ZnO nanostructures of diverse morphology at temperature range 200 – 500 °C via using zinc acetylacetonate as a single source precursor is reported. Distinctive feature is that the nanostructures morphology changes systematically with the temperature, driven by ZnO crystal planes anisotropy and obeying the crystal growth theory. Within the temperature range 200 – 500 °C via applying the varying precursor's pressure the nanostructures undergo the evolution of their shape from the polycrystalline blocks of nanocrystals to the ordered textured array of the nanorods. At low precursors pressure it was observed, that the substrate of low mismatch tend to be overgrown epitaxially by ZnO nanocrystals, while large mismatched substrate provides discrete growth of ZnO nanocrystals of basic (primitive) shape. Due to the demonstrated features, the grown nanostructures may have the possible applications as a low scale adsorbents and catalysts; nanosensors or field emitters; optical waveguide splitters or recombiners; nanotools; nanosized LEDs.

Acknowledgements

Swedish Research Link (SRL-VR) 2009-6427 “ZnO Nano Structures for Energy Saving Light Emitters” (2010 – 2012) and Linné grant in IFM LiU are acknowledged for the support.

References

- [1] Ü. Özgür, Ya. I. Alivov, C. Liu, A. Teke, M. A. Reshchikov, S. Doğan, V. Avrutin, S.-J. Cho, and H. Morkoç, A comprehensive review of ZnO materials and devices // J. Appl. Phys. 98 (2005) 041301
- [2] V. Khranovskyy, G. R. Yazdi, G. Lashkarev, A. Ulyashin, and R. Yakimova, Investigation of ZnO as a perspective material for photonics // Phys. Stat. Sol. (a) 205 (2008) 144
- [3] V. Khranovskyy, J. Eriksson, A. Lloyd-Spetz, L. Hultman and Rositza Yakimova, Effect of oxygen exposure on the electrical conductivity and gas sensitivity of nanostructured ZnO films // Thin Solid Films 517 (2009) 2073-2078
- [4] A. Evtukh, V. Litovchenko, M. Semenenko, V. Karpyna, G. Lashkarev, V. Lazorenko, V. Khranovskyy, L. Kopylova, Yu. Piryatinsky, Peculiarities of electron

field emission from ZnO nanocrystals and nanostructured films // Superlattices and Microstructures 42 (2007) 451-460

- [5] V. A. Karpyna, A. A. Evtukh, M. O. Semenenko, V. I. Lazorenko, G. V. Lashkarev, V. D. Khranovskyy, R. Yakimova, D. A. Fedorchenko, Electron field emission from ZnO self-organized nanostructures and doped ZnO:Ga nanostructured films // Microelectronics Journal 40 (2009) 229-231
- [6] M. Willander, O. Nur, Q. X. Zhao, L. L. Yang, M. Lorenz, B. Q. Cao, J. Z. Perez, C. Czekalla, G. Zimmermann, M. Grundmann, A. Bakin, A. Behrends, M. Al-Suleiman, A. El-Shaer, A. Che Mofor, B. Postels, A. Waag, N. Boukos, A. Travlos, H. S. Kwack, J. Guinard and D. Le Si Dang, Zinc oxide nanorod based photonic devices: recent progress in growth, light emitting diodes and lasers // Nanotechnology 20 (2009) 332001
- [7] A. Djurisic, A. Ng, X. Chen, ZnO nanostructures for optoelectronics: Material properties and device applications // Progress in Quantum Electronics 34 (2010) 191–259
- [8] G. Lashkarev, V. Karpina, V. Lazorenko, A. Ievtushenko, I. Shtepliuk and V. Khranovskyy, Properties of ZnO at low and moderate temperatures // Low Temperature Physics 37 (2011) 226
- [9] V. Khranovskyy, I. Tsiaoussis, L. Hultman and R. Yakimova, Selective homoepitaxial growth and luminescent properties of ZnO Nanopillars // Nanotechnology 22 (2011) 185603
- [10] V. Khranovskyy, I. Tsiaoussis, L. A. Larsson, P. O. Holtz and Rositza Yakimova, Nanointegration of ZnO with Si and SiC // Physica B 404 (2009) 4359 - 4363
- [11] L. Xu, Y.-L.g Hu, C. Pelligra, C.-H. Chen, L. Jin, H. Huang, S. Sithambaram, M. Aindow, R. Joesten and S.L. Suib, ZnO with Different Morphologies Synthesized by Solvothermal Methods for Enhanced Photocatalytic Activity // Chem. Mater. 21 (2009) 2885
- [12] J. B. Baxter, E. S. Aydil, Epitaxial growth of ZnO nanowires on a- and c-plane sapphire // J. Cryst. Growth 274 (2005) 407–411
- [13] V. Khranovskyy, A. Ulyashin, G. Lashkarev, B.G. Svensson, R. Yakimova, Morphology, electrical and optical properties of undoped ZnO layers deposited on silicon substrates by PEMOCVD // Thin Solid Films 516 (2008) 1396-1400
- [14] www.sigmaaldrich.com
- [15] D. Shenai-Khatkhate, R. Goyette, R. Dicarlo, G. Dripps, Environment, health and safety issues for sources used in MOVPE growth of compound semiconductors // J. Cryst. Growth 272 (2004) 816-821.
- [16] G. Rudolph, M. C. Henry, The Thermal Decomposition of Zinc Acetylacetonate Hydrate // Inorg. Chem. 3 (1964) 1317–1318
- [17] A. J. C. Fiddes, K. Durose, A. W. Brinkman, J. Woods, P. D. Coates, A. J. Banister, Preparation of ZnO films by spray pyrolysis // J. Cryst. Growth 159 (1996) 210-213

- [18] T Arii and A Kishi, The effect of humidity on thermal decomposition of zinc acetylacetonate monohydrate // *J. Therm. Anal. Calorim.* 83 (2006) 253
- [19] C. Fauteux, R. Longtin, J. Pegna, and D. Therriault, Fast Synthesis of ZnO Nanostructures by Laser-Induced Decomposition of Zinc Acetylacetonate // *Inorg. Chem.* 46 (2007) 11036
- [20] J.-J. Wu and S.-C. Liu, Low-Temperature Growth of Well-Aligned ZnO Nanorods by Chemical Vapor Deposition // *Adv. Mat.* 14 (2002) 215
- [21] V Khranovskyy, U Grossner, O Nilsen, V Lazorenko, G V Lashkarev, B G Svensson, R Yakimova, Structural and morphological properties of ZnO:Ga thin films // *Thin Solid Films* 515 (2006) 472-476
- [22] V. Khranovskyy, U. Grossner, V. Lazorenko, G. Lashkarev, B.G. Svensson, R. Yakimova, PEMOCVD of ZnO thin films, doped by Ga and some of their properties // *Superlattices and Microstructures* 39 (2007) 275-281
- [23] V. Khranovskyy, R. Minikayev, S. Trushkin, G. Lashkarev, V.I Lazorenko, U. Grossner, W. Paszkowicz, A.j Suchocki, B. G. Svensson and Rositza Yakimova, Improvement of ZnO thin film properties by application of ZnO buffer layers // *J. Cryst. Growth* 308 (2007) 93-98
- [24] V. Khranovskyy, I. Tsiaoussis, G. R. Yazdi, L. Hultman and R. Yakimova, Heteroepitaxial ZnO nanohexagons on p-type SiC // *Journal of Crystal Growth*, 312 (2010) 327 – 332
- [25] N. Fujimura, T. Nishihara, S. Goto, J. Xu, T. Ito, Control of preferred orientation for ZnO_x films: control of self-texture // *J. Cryst. Growth* 130 (1993) 269-279
- [26] V. Khranovskyy, U. Grossner, V. Lazorenko, G. Lashkarev, B. G. Svensson, R. Yakimova, Study of annealing influence on electrical and morphological properties of ZnO:Ga thin films // *Phys. Stat. Sol. (c)* 3 (2006) 780–784
- [27] Schüth, F., Sing, K. S. W. & Weitkamp, J. *Handbook of Porous Solids*(Wiley-VCH, 2002)
- [28] J. Eriksson, V. Khranovskyy, F. Söderlind, P.-O. Käll, R. Yakimova, A. Lloyd Spetz , ZnO nanoparticles or ZnO films, a comparison of the gas sensing capabilities // *Sensors and Actuators B* 137 (2009) 94–102
- [29] R. Yakimova, G. Steinhoff, R.M. Petoral Jr., C. Vahlberg, V. Khranovskyy, G.R. Yazdi, K. Uvdal, A. Lloyd Spetz, Novel material concepts of transducers for chemical and biosensors // *Biosensors and Bioelectronics* 22 (2007) 2780-2785.

Figure captions

Figure 1. The XRD patterns of ZnO nanostructures grown at set 1 conditions and respective substrate temperature ranges: a - corrals (200 – 240 °C); b - cabbages (240 – 280 °C); c - porous hexagons (280 - 320 °C); d - bundles (320 – 365 °C); e - sheaves (365 – 415 °C); f - open sheaves (415 – 525 °C). The respective reflections of the crystallographic planes are indicated. The substrate peak is marked as “*”.

Figure 2. The SEM images of ZnO nanostructures grown at set 1 conditions and respective substrate temperature ranges: a - corrals (200 – 240 °C); b - cabbages (240 – 280 °C); c - porous hexagons (280 - 320 °C); d - bundles (320 – 365 °C); e - sheaves (365 – 415 °C); f - open sheaves (415 – 525 °C). The insets represent respective enlarged images of the features.

Figure 3. ZnO nanostructures, grown at low precursor pressure on Si (a) and SiC (b) at 450 °C.

Table 1. Description of the morphology shape and structural features of ZnO nanostructures depend on the growth temperature

Growth temperature range, °C	$2\theta_{(hkl)}$, (degrees)	Crystal planes (<i>h k l</i>)	XRD FWHM, (degrees)	XRD Intensity (<i>h k l</i>), a. u.	Morphology	Characteristic size
200 – 240	31.76	(100)	0.3	45	Corals	1 – 2 μm
	34.47	(002)	0.2	954		
	36.29	(101)	0.24	80		
240 – 280	32.5	(100)	0.21	68	Cabbages	1.5 – 2 μm / pores around 15 – 40 nm
	34.46	(002)	0.16	1366		
	36.33	(101)	0.19	6		
280 – 320	34.48	(002)	0.14	1761	Porous hexagons	1.5 – 2 μm / pores around 20 – 80 nm
	36.3	(101)	0.18	22		
320 – 365	34.48	(002)	0.23	1426	Bundles	1.5 – 2 μm / 30 – 50 nm at the tips
365 – 415	34.48	(002)	0.24	1321	Sheaves	1 – 1.2 μm / 30 – 40 nm
415 – 525	34.466	(002)	0.27	1033	Open sheaves	1 μm / 20 – 30 nm